

Combinatorial Screening of Polymeric Sensing Materials Using RFID Sensors: Combined Effects of Plasticizers and Temperature

Radislav A. Potyrailo,* Cheryl Surman, and William G. Morris

General Electric Global Research Center, Niskayuna, NY

Received January 1, 2009

Recently, we have developed battery-free, passive RFID chemical and biological sensors that are attractive in diverse applications where sensor performance is needed at a low cost and when battery-free operation is critical. In this study, we apply this attractive low-cost sensing platform for the combinatorial screening of formulated sensing materials. As a model system, a 6×8 array of polymer-coated RFID sensors was constructed to study the combined effects of polymeric plasticizers and annealing temperature. A solid polymer electrolyte Nafion was formulated with five different phthalate plasticizers: dimethyl phthalate, butyl benzyl phthalate, di-(2-ethylhexyl) phthalate, dicapryl phthalate, and diisotridecyl phthalate. These sensing film formulations and control sensing films without a phthalate plasticizer were deposited onto 9-mm diameter RFID sensors, exposed to eight temperatures ranging from 40 to 140 °C using a gradient temperature heater, and evaluated for their response stability and gas-selectivity response patterns. This study demonstrated that our RFID-based sensing approach permits rapid cost-effective combinatorial screening of dielectric properties of sensing materials.

1. Introduction

Radio frequency identification (RFID) tags have found their broad applicability, when there is a need for tracking of different types of assets. This capability of RFID tags is provided by the unique factory programmed 64- or 96-bit serial number of the RFID that allows tracking of individual items as opposed to just the manufacturer and class of products, as conventional barcodes do today. Examples of demanding applications of passive (battery-free) RFID tags include product authentication, ticketing and access control, lifetime item identification, animal and specimen identification, baggage handling, and many others.^{1,2} RFID tags have also been employed for tracking of combinatorial chemistry reaction products.³ For these and many other applications, the attractiveness of passive RFID tags come from their small size of being only several millimeters and low cost of being less than \$1.⁴

Recently, we adapted ubiquitous and cost-effective passive RFID tags for chemical sensing.⁵ By applying a sensing material onto the resonant antenna of the RFID tag and measuring the complex impedance of the RFID resonant antenna it was possible to correlate impedance response to chemical properties of interest. The operation principle of developed RFID sensors is illustrated in Figure 1. Upon reading of the RFID sensor with a pickup coil, the electromagnetic field generated in the RFID sensor antenna extends out from the plane of the RFID sensor (Figure 1A) and is affected by the dielectric property of an ambient environment providing the opportunity for sensing of physical, chemical, and biological parameters.

When a sensing film is deposited onto the resonant antenna (Figure 1B), the analyte-induced changes in the dielectric and dimensional properties of this sensing film affect the complex impedance of the antenna circuit through the changes in film resistance and capacitance between the antenna turns. Such changes provide selectivity in response of an individual RFID sensor and provide the opportunity to replace a whole array of conventional sensors with a single RFID sensor.⁵ For this selective analyte quantitation using individual RFID sensors, complex impedance spectra of the resonant antenna are measured. Several parameters from the measured real and imaginary portions of the complex impedance are further calculated as shown in Figure 1C. By applying multivariate analysis of the full complex impedance spectra or the calculated parameters, quantitation of analytes, and rejection of interferences is performed with individual RFID sensors.

Temperature effects are important at all stages of sensor fabrication and end-use. Understanding of temperature effects can provide ability to build robust temperature-corrected transfer functions of sensor performance in order to preserve response sensitivity, response selectivity, and response baseline stability.^{6–9} Table 1 provides several representative examples of key temperature-induced affects during the formulation and deposition of sensing material, sensor conditioning before calibration, sensor storage before the use, and sensor end-use.

In this study, we apply RFID sensors for the combinatorial screening of sensing materials to evaluate combined effects of polymeric plasticizers and annealing temperature. As a model system, a 6×8 array of polymer-coated RFID sensors was constructed. A solid polymer electrolyte Nafion was formulated with five types of phthalate

* To whom correspondence should be addressed. E-mail: Potyrailo@crd.ge.com.

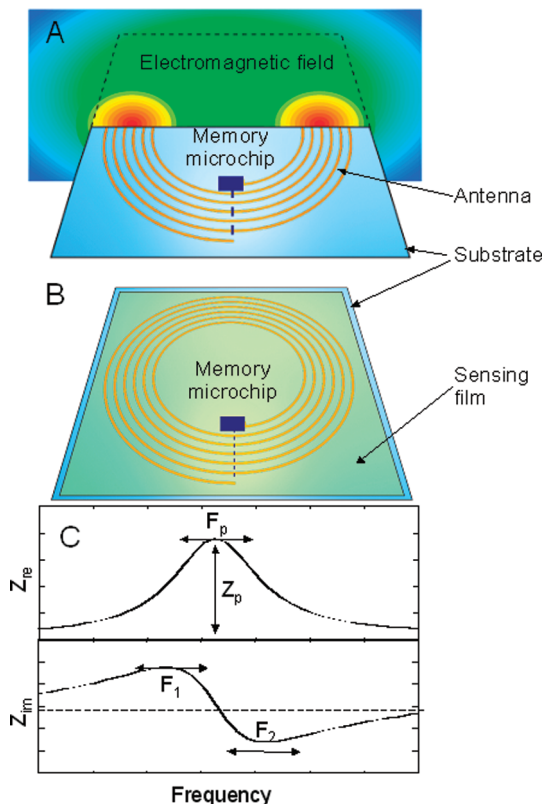


Figure 1. Operation principle of developed passive RFID chemical sensors. (A) Schematic of the spatial distribution of the electromagnetic field in the sensor antenna generated by inductive coupling with a pick up coil. (B) Sensing film deposited onto the resonant antenna. Analyte-induced changes in the film affect the complex impedance of the antenna circuit through the changes in film resistance and capacitance between the antenna turns. (C) Measured complex impedance spectrum (real part Z_{re} and imaginary part Z_{im} of complex impedance) and representative parameters for multivariate analysis: F_p and Z_p are the frequency and magnitude of the maximum of the real part of the complex impedance, respectively; F_1 and F_2 are the resonant and antiresonant frequencies of the imaginary part of the complex impedance, respectively.

plasticizers. These sensing film formulations and control sensing films without a phthalate plasticizer were deposited onto RFID sensors, exposed to eight temperatures ranging from 40 to 140 °C using a gradient temperature heater, and evaluated for their response stability and gas-selectivity response patterns. This study demonstrated that our RFID-based sensing approach permits rapid cost-effective combinatorial screening of dielectric properties of sensing materials.

2. Experimental Section

Sensing materials formulations included a base polymer with several types of phthalate plasticizers. The base polymer was a solid polymer electrolyte Nafion (Aldrich), a copolymer of tetrafluoroethylene and sulfonyl fluoride vinyl ether (see Figure 2). The chemical structures of employed phthalate plasticizers are shown in Figure 3. Nafion was supplied as a 5% wt. solution in lower aliphatic alcohols and water. Plasticizers were dissolved in the Nafion solution to yield a 10% wt plasticizer solution.

Table 1. Representative Examples of Key Temperature-Induced Affects at Different Stages of Sensor Fabrication and End Use

stage of fabrication or end-use of sensing material	examples of key temperature-induced effects
formulation/deposition	solubility of formulation components film morphology/heterogeneity
conditioning before calibration	stabilization of formulation components
shelf storage	aging of formulation components
end use	analyte response slope selectivity pattern between several analytes selectivity pattern between analyte(s) and interferences sensing material/transducer interface

For deposition of sensing films, a small volume (10–30 μL) of solutions was applied onto the surface of RFID tags by drop-coating and dried in air overnight. Temperature annealing of the sensing films was performed in ambient air by arranging the 6×8 array of films (six film compositions \times eight temperatures) on a home-built gradient temperature heater. The heater generated a temperature gradient from 40 to 140 °C.

RFID sensors were constructed from passive 13.56 MHz RFID tags from TagSys (Doylestown, PA). The interrogation of RFID sensors in the array was done with a single transmitter (pick-up coil) positioned on an X–Y translation stage and connected to a network analyzer (Model E5062A, Agilent Technologies, Inc. Santa Clara, CA). Digital data readings from the IC memory chips of RFID sensors were performed using a multistandard RFID Reader/Writer evaluation module (Model TRF7960 Evalu-

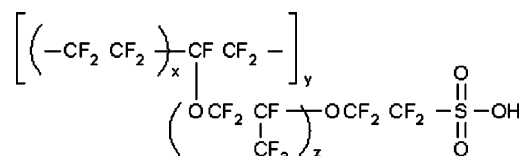


Figure 2. Chemical structure of Nafion polymer employed as a sensing matrix material in this study.

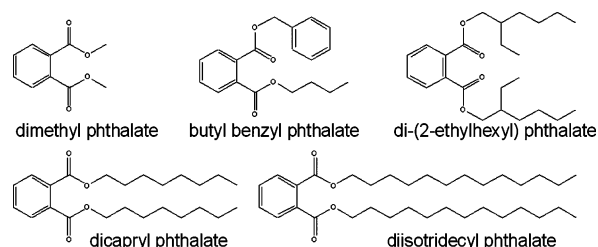


Figure 3. Chemical structures of employed phthalate plasticizers.

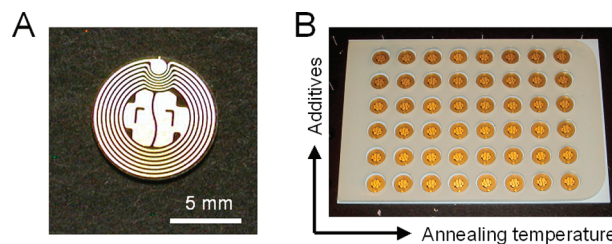


Figure 4. Combinatorial screening of sensing film compositions using passive RFID sensors. (A) Photo of an employed RFID sensor (memory chip type = I*CODE1, memory chip ID = 0900 000 457D 5E12). (B) Photo of an array of 48 RFID sensors prepared for temperature-gradient evaluations of response of Nafion/phthalates compositions.

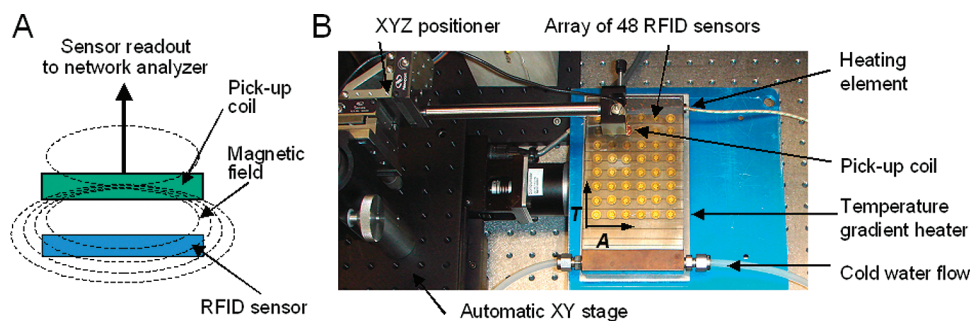


Figure 5. Experimental system for the combinatorial screening of sensing film compositions using passive RFID sensors. (A) Schematic of the signal generation in an RFID sensor through the inductive coupling between the pick up coil and RFID sensor. (B) General view of the experimental system with the 6×8 RFID sensor array positioned on a gradient temperature heater.

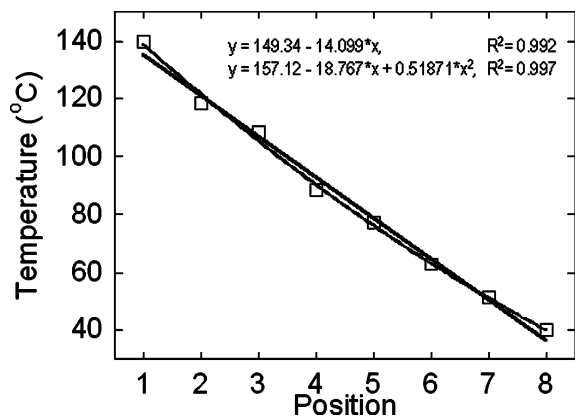


Figure 6. Temperature response of an in-house built heater for temperature studies of materials arranged in standard well plate formats.

ation Module, Texas Instruments). Measurements of the complex impedance of RFID sensors were performed with the network analyzer under computer control. For the evaluation of the stability of vapor responses, two analytes were tested at ambient laboratory temperature. These analytes included water (H_2O) and acetonitrile (ACN) vapors, all at a concentration (partial pressure) of 0.4 of the saturated vapor pressure (P_0). The vapor concentrations were produced under a computer control by bubbling nitrogen through pure solvents and further diluting the resulting vapors with nitrogen.

3. Results and Discussion

The employed RFID sensors are shown in Figure 4. RFID sensors were 9 mm in diameter (see Figure 4A) and were arranged as a 6×8 sensor array (Figure 4B) with six material compositions and eight sensors of the same composition for exposures to eight temperatures. Both analog and digital data can be read from these sensors. The digital data can be written into and read from the 13.56 MHz integrated circuit (IC) memory chip of the RFID tag. This IC memory chip can store sensor calibrations and user-defined information. The 6×8 RFID sensor array was arranged on a gradient temperature heater to generate a temperature gradient from 40 to 140 °C.

The constructed experimental setup is shown in Figure 5. Operation of our RFID sensors can be described using inductive signal coupling effects between a pick up coil and the RFID sensor^{1,2} as shown in Figure 5A. To probe all sensors in the 6×8 array, the single pick up coil was arranged on an automatic X–Y stage. The 9-mm sensor diameter permitted scanning of the sensor array with a single pick-up coil without interferences from neighbor sensors. The gradient heater design provided the opportunity for temperature studies of materials arranged in standard well plate formats of $\sim 90 \times 120$ mm. Depending on the plate layout, materials can be arranged in 24-, 48-, 96-, and 384-well plate libraries.

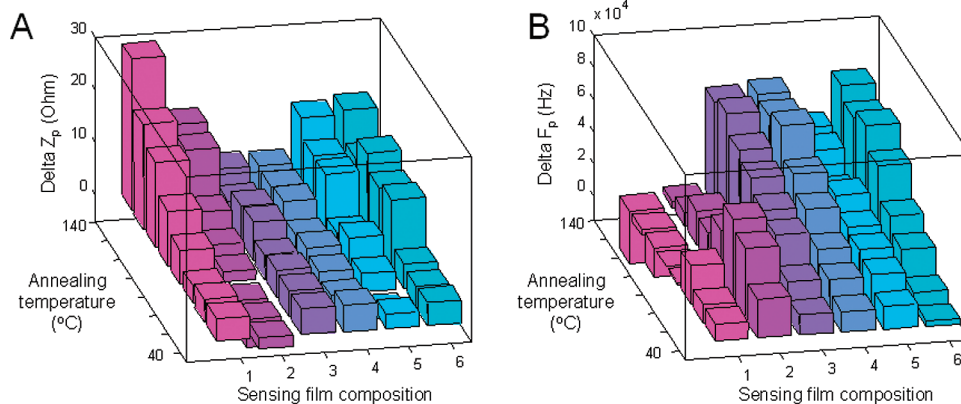


Figure 7. Results of temperature annealing of 48-sensing film library in air plotted as (A) impedance ΔZ_p and (B) frequency ΔF_p response after and before the annealing from each sensor as a function of annealing temperature and material composition. Nafion sensing film compositions: 1, control without plasticizer; 2, dimethyl phthalate; 3, butyl benzyl phthalate; 4, di-(2-ethylhexyl) phthalate; 5, dicapryl phthalate; 6, diisotridecyl phthalate.

Table 2. Parameters and Temperature Stability (As Boiling Point^{22,23}) of Nafion/Phthalate Sensing Film Compositions

composition	plasticizer type	boiling point, °C	sensor response ΔZ_p (ohm)	sensor response ΔF_p (Hz)
1	control (without plasticizer)		28.781	-32590
2	dimethyl phthalate	284	15.667	3940
3	butyl benzyl phthalate	370	6.781	64200
4	di-(2-ethylhexyl) phthalate	384	6.715	66880
5	dicapryl phthalate	230	15.351	44020
6	diisotridecyl phthalate	260	16.375	68880

The temperature response of the heater with the 6×8 arrays of RFID sensors was calibrated using thermocouples positioned along the temperature gradient. Results of temperature mapping of the heater performance are illustrated in Figure 6. Similar to other heater designs, this heater had an almost linear temperature distribution as determined from the correlation coefficient ($R^2 = 0.992$) for a linear fit. The correlation coefficient for a quadratic fit was only negligibly better ($R^2 = 0.997$).

In sensing materials based on solid polymer electrolytes, conductivity depends on ionic mobility rather than electron mobility. Modifications of selectivity patterns of this type of sensing materials in response to different analytes have been achieved by formulating them with different functional additives. For example, Nafion films have been formulated with hydrogels,¹⁰ ionic liquids,¹¹ salts,¹² surfactants,¹³ and many other additives. Phthalates or phthalate esters are esters of phthalic acid and are used as plasticizers of different polymers.^{14–16} In sensing applications, phthalate plasticizers were used previously

in different polymeric films to induce the diversity in vapor response.^{17–20} In this study, we formulated different phthalate plasticizers in Nafion at 10% vol to induce selectivity in vapor response and to study long-term stability of these sensing films.

Temperature annealing of six compositions of sensing films (1–6) was performed in air at eight temperatures ranging from 40 to 140 °C. This temperature range was selected because Nafion is a glassy polymer at room temperature with the glass transition temperature of its acid form at ~ 110 °C and of its salts at ~ 220 °C.²¹ After temperature annealing for 1 h, the impedance response difference ΔZ_p and frequency response difference ΔF_p before and after the annealing from each sensor in air was calculated (see Figure 7). The smallest ΔZ_p and ΔF_p responses were associated with the most stable film composition after annealing. Table 2^{22,23} compares the values of boiling point for each phthalate plasticizer used in this study with ΔZ_p and ΔF_p responses from sensors exposed to the highest temperature of 140 °C.

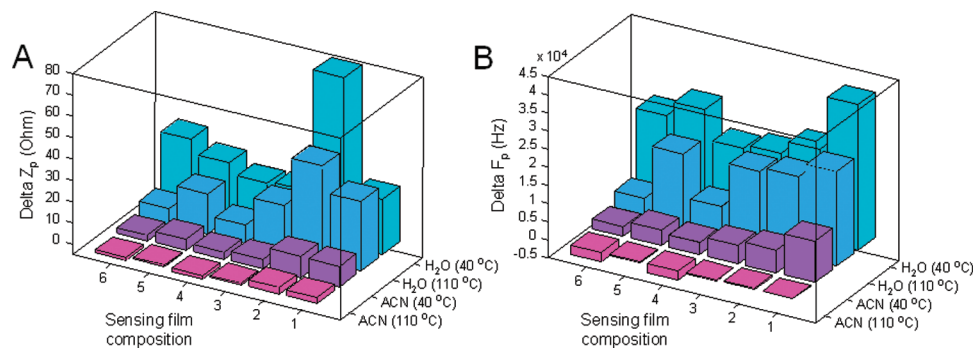


Figure 8. RFID sensors response to water (H₂O) and acetonitrile (ACN) vapors after annealing at different temperatures (40 and 110 °C): (A) Z_p response and (B) F_p response. Nafion sensing film compositions: 1, control without plasticizer; 2, dimethyl phthalate; 3, butyl benzyl phthalate; 4, di-(2-ethylhexyl) phthalate; 5, dicapryl phthalate; 6, diisotridecyl phthalate.

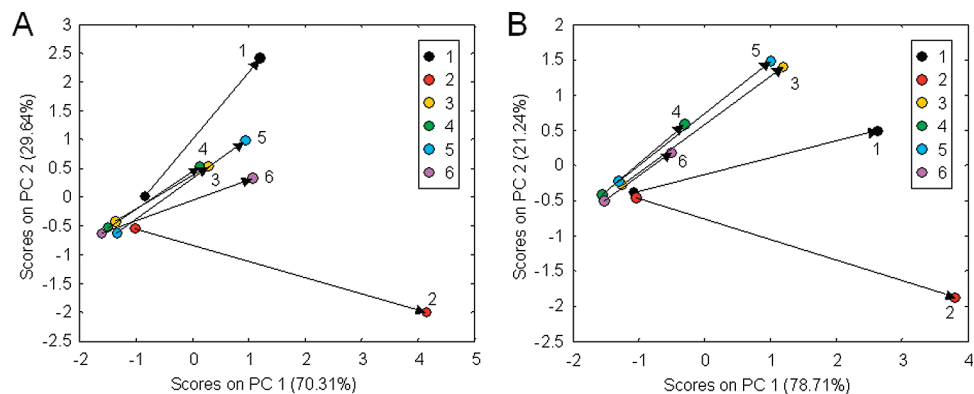


Figure 9. Results of principal components analysis of F_1 , F_2 , F_p , and Z_p responses of RFID sensors with sensing films 1–6 to H₂O and ACN vapors upon annealing at (A) 40 and (B) 110 °C. Arrows illustrate the H₂O–ACN Euclidean distances and the response direction of sensing films 1–6. Nafion sensing film compositions: 1, control without plasticizer; 2, dimethyl phthalate; 3, butyl benzyl phthalate; 4, di-(2-ethylhexyl) phthalate; 5, dicapryl phthalate; 6, diisotridecyl phthalate.

To evaluate temperature effects on sensor response selectivity, the 6×8 array of temperature-annealed sensing films was further exposed to H₂O and ACN vapors. Acetonitrile was selected as a simulant for blood chemical warfare agents (CWAs)²⁴ while water vapor was selected as an interference. In these experiments, the partial pressures of H₂O and ACN vapors were 0.4 of the saturated vapor pressure P_0 . These partial pressures corresponded to 1.3×10^4 ppm and 4.7×10^4 ppm of H₂O and ACN vapors, respectively. Our earlier developed Nafion-coated RFID sensors demonstrated subppm detection limits of H₂O vapor and ppm detection limits of ACN vapor.⁵

Nafion sensing films were used previously for humidity^{25,26} and organic vapors²⁷ detection. Conductance and dielectric properties of Nafion have been shown to be vapor-dependent.^{28,29} Figure 8 shows representative ΔZ_p and ΔF_p responses to H₂O and ACN upon annealing at two temperatures, 40 and 110 °C. The response of all sensing materials to H₂O was stronger than to ACN. This difference can be attributed to the difference in dielectric constants of H₂O ($\epsilon_{\text{H}_2\text{O}} = 80$) and ACN ($\epsilon_{\text{ACN}} = 37$).

The patterns of response of sensing films to H₂O and ACN vapors upon annealing at 40 and 110 °C were examined using principal components analysis (PCA).³⁰ PCA is a multivariate data analysis tool that projects the data set onto a subspace of lower dimensionality with removed collinearity. PCA achieves this objective by explaining the variance of the data matrix in terms of the weighted sums of the original variables with no significant loss of information. These weighted sums of the original variables are called principal components (PCs). Results of the PCA multivariate analysis of multiparameter (ΔF_1 , ΔF_2 , ΔF_p , and ΔZ_p) response of RFID sensors with sensing films 1–6 to H₂O and ACN upon annealing at 40 and 110 °C are presented in Figure 9. Prior to PCA, the data was appropriately preprocessed by autoscaling. Arrows illustrate the H₂O–ACN Euclidean distances and the response direction of sensing films 1–6. Arrows begin at the response of the sensing film to ACN and end at the response of the sensing film to H₂O. While many distance metrics have been reported for use in cluster analysis, the Euclidean distance is the most commonly used.³⁰ The length of the arrows (the H₂O–ACN Euclidean distances) indicate response diversity of sensing films 1–6 to H₂O and ACN. The larger the Euclidean distance, the better the sensing material is in its response diversity to H₂O and ACN.

The first two PCs of the PCA models of responses of sensing films 1–6 to H₂O and ACN include more than 99% of the total variance from the data sets (Figure 9), indicating that using only two PCs is sufficient for the examination of materials diversity of the response to H₂O and ACN. The scores plots of the first two PCs can be used to draw several conclusions about the effects of plasticizers and temperature on the diversity of the response to H₂O and ACN. First, different annealing temperature alters diversity of sensing films 1–6 either with a positive or a negative effect as indicated by the increase or decrease of the H₂O–ACN Euclidean distances. Second, different plasticizers affect the response diversity to a different extend,

however Nafion sensing films formulated with the dimethyl phthalate plasticizer improve response diversity of the sensing films to H₂O and ACN.

4. Conclusion

This general approach of RFID sensing opens numerous opportunities where the high quality of sensor performance is needed at low cost and when battery-free operation is critical. This study demonstrated that these passive RFID sensors are very attractive for the rapid cost-effective combinatorial screening of dielectric properties of sensing materials. This demonstrated approach provided the capability of using conventional passive RFID tags as high-performance transducers for rapid studies of stabilization effects of plasticizers and temperature annealing.

While the combinatorial screening data clearly showed the effects of all plasticizers and annealing temperature on the H₂O response magnitude and on the H₂O/ACN response pattern, our work is in progress to understand these complex relations between the plasticizer structure and its function in a formulated polymer upon temperature annealing.

Acknowledgment. This work has been supported by GE Corporate long-term research funds. Authors are thankful to Bill Flanagan for the design of the gradient heater used in this work.

References and Notes

- (1) Finkeneller, K. *RFID Handbook. Fundamentals and Applications in Contactless Smart Cards and Identification*, 2 ed.; Wiley: Hoboken, NJ, 2003.
- (2) Lehpamer, H. *RFID Design Principles*; Artech House: Norwood, MA, 2008.
- (3) Nicolaou, K. C.; Xiao, X.-Y.; Parandoosh, Z.; Senyei, A.; Nova, M. P. *Angew. Chem., Int. Ed.* **1995**, *34*, 2289–2291.
- (4) Roberti, M. *RFID J.* **2006**, 2295 <http://www.rfidjournal.com/article/articleview/2295>.
- (5) Potyrailo, R. A.; Morris, W. G. *Anal. Chem.* **2007**, *79*, 45–51.
- (6) Potyrailo, R. A. *Proc. SPIE* **1993**, 2069, 76–84.
- (7) Potyrailo, R. A.; Golubkov, S. P.; Borsuk, P. S.; Talanchuk, P. M.; Novoselov, E. F. *Analyst* **1994**, *119*, 443–448.
- (8) Potyrailo, R. A.; Sivavec, T. M.; Bracco, A. A. *Proc. SPIE* **1999**, 3856, 140–147.
- (9) Potyrailo, R. A.; Morris, W. G. *Rev. Sci. Instrum.* **2007**, *78*, 072214.
- (10) Madaras, M. B.; Buck, R. P. *Anal. Chem.* **1996**, *68*, 3832–3839.
- (11) Bennett, M. D.; Leo, D. J. *Sens. Actuators A* **2004**, *115*, 79–90.
- (12) DeLongchamp, D. M.; Hammond, P. T. *Chem. Mater.* **2003**, *15*, 1165–1173.
- (13) Singh, K.; Shahi, V. K. *J. Membr. Sci.* **1998**, *140*, 51–56.
- (14) Etchenique, R.; Weisz, A. D. *J. Appl. Phys.* **1999**, *86*, 1994–2000.
- (15) Jose, B.; Ryu, J. H.; Kim, Y. J.; Kim, H.; Kang, Y. S.; Lee, S. D.; Kim, H. S. *Chem. Mater.* **2002**, *14*, 2134–2139.
- (16) Song, M.-K.; Kim, Y.-T.; Hwang, J.-S.; Ha, H. Y.; Rhee, H.-W. *Electrochem. Solid-State Lett.* **2004**, *7*, A127–A130.
- (17) Buhlmann, K.; Schlatt, B.; Cammann, K.; Shulga, A. *Sens. Actuators B* **1998**, *49*, 156–165.
- (18) Matzger, A. J.; Lawrence, C. E.; Grubbs, R. H.; Lewis, N. S. *J. Comb. Chem.* **2000**, *2*, 301–304.
- (19) Burl, M. C.; Sisk, B. C.; Vaid, T. P.; Lewis, N. S. *Sens. Actuators B* **2002**, *87*, 130–149.

- (20) Kim, Y. S.; Ha, S.-C.; Yang, Y.; Kim, Y. J.; Cho, S. M.; Yang, H.; Kim, Y. T. *Sens. Actuators B* **2005**, *108*, 285–291.
- (21) Yeo, S. C.; Eisenberg, A. *J. Appl. Polym. Sci.* **1977**, *21*, 875–898.
- (22) Wypych, A. *Plasticizers Database*; 2nd electronic ed.; ChemTec Publishing: Toronto, ON, Canada, 2004.
- (23) Speight, J. G., Ed. *Lange's Handbook of Chemistry*, 15th ed.; McGraw-Hill: New York, NY, 2005.
- (24) Lee, W. S.; Lee, S. C.; Lee, S. J.; Lee, D. D.; Huh, J. S.; Jun, H. K.; Kim, J. C. *Sens. Actuators B* **2005**, *108*, 148–153.
- (25) Feng, C.-D.; Sun, S.-L.; Wang, H.; Segre, C. U.; Stetter, J. R. *Sens. Actuators B* **1997**, *40*, 217–222.
- (26) Tailoka, F.; Fray, D. J.; Kumar, R. V. *Solid State Ionics* **2003**, *161*, 267–277.
- (27) Sun, L.-X.; Okada, T. *J. Membr. Sci.* **2001**, *183*, 213–221.
- (28) Cappadonia, M.; Erning, J. W.; Niaki, S. M. S.; Stimming, U. *Solid State Ionics* **1995**, *77*, 65–69.
- (29) Wintersgill, M. C.; Fontanella, J. J. *Electrochim. Acta* **1998**, *43*, 1533–1538.
- (30) Jurs, P. C.; Bakken, G. A.; McClelland, H. E. *Chem. Rev.* **2000**, *100*, 2649–2678.

CC900001N